Model and Design of a Four-Stage Thermoacoustic Electricity Generator with Two Push-Pull Linear Alternators

Ahmed Hamood[1], Artur J. Jaworski[1, *], and Xiaoan Mao[1]

[1]Faculty of Engineering, University of Leeds, Woodhouse Lane, Leeds LS2 9JT, United Kingdom

Abstract. Recent work of the authors on a two-stage thermoacoustic electricity generator with a "push-pull" linear alternator has led to further investigations of multi-stage thermoacoustic engines. The investigation started with proposing a new feedback loop to reduce the length and the volume of the two-stage engine. The use of acoustic inertance-compliance reduced the engine total length from 16.1 m to 7.5 m and maintained the performance. A four-stage traveling wave thermoacoustic engine is considered working as an electricity generator with two push-pull linear alternators. The proposed engine considered the thermoacoustic core geometries of the two-stage engine. The engine consists of four identical quarter-wave stages connected in series to form one wave length thermoacoustic engine. The engine compact model is 5.2 m in length. Using pressurized helium at 28 bar as a working gas, the simulation showed that engine generates 261 W of electricity using heat source at exhaust gases temperature of the IC engines. The simulation has been done using DeltaEC package. The research shows that the four-stage engine does not require a compliance in the feedback loop as the core itself acts as a compliance. The results presented in this paper demonstrate that four-stage thermoacoustic engine has a good potential for waste heat recovery and inexpensive electricity generation.

1 Introduction

Day by day, the demand for energy rises all over the [†]world. In recent years a lot of environmental impacts have been discovered and proven as being caused by power generation technologies. This creates a thoughtful approach towards clean and environmentally friendly technologies. Thermoacoustic power generation technology could be considered as one such technology. Sound waves in fluids are normally regarded as coupled oscillations of pressure and velocity; however these are also associated with temperature oscillations. These temperature changes are too small to be noticed in the

* Corresponding author: a.j.jaworski@leeds.ac.uk

typical sound propagation processes in air at atmospheric pressure. However, in highly pressurised gases (e.g. at pressures of the order of 30-60 bar) and at high acoustic intensity the temperature changes become significant. The temperature effects can be utilised for energy conversion processes when the acoustic wave propagates next to the solid body. Using a sound source, a temperature gradient can be built up in the solid. Imposing a temperature gradient on the solid may lead to the generation of acoustic power. These processes form the back-bone of thermoacoustic technologies [1]. Thus, thermoacoustics is the interaction between thermodynamics and acoustics in the fluid medium inside a special solid configuration within acoustic resonance conditions.

Internal combustion engines are heat engines that combust fuel with an oxidizer inside the engine. The thermal energy released by burning the fuel will leave the engine as thermal energy rejected by the cooling water, exhaust gases, miscellaneous losses or as brake power. Taymaz [2] reported results for the heat balance of a standard four stroke diesel engine with a capacity of 6.0 litres. The heat rejected to the exhaust system ranged from 24% to 29% of the total energy released from the fuel depending on the engine load. The availability of this large amount of waste energy gives the potential to harvest waste heat and convert it to useful work. Johnson [3] outlined the technologies to generate cooling power from waste heat from exhaust gases. Thermoacoustic technology has been listed as one of the four vital technologies. Later on, Jadhao and Thombare [4] highlighted thermoacoustic technology as a direct electricity generator in their review of internal combustion engine exhaust gas heat recovery. The advantages of using thermoacoustic technology electricity generator as the system is elegant, reliable, low cost, environmentally safe and has no moving parts (in thermodynamic section). The disadvantages were low efficiency and power density.

The first looped tube thermoacoustic engine was presented by Yazaki et al. [5]. The configuration of travelling wave engine was a one wavelength loop which contained the thermoacoustic core at a specific location. The experimental results showed that the travelling wave engine uses the temperature gradient at the regenerator to perform as an acoustic amplifier. Kitadani et al. [6] investigated the electricity generation from a looped tube engine. A loudspeaker was connected within the loop to convert the acoustic power to electricity and was placed at the end of a branch optimised to be a quarter wavelength. The dependence of sound amplification on the phase difference between the acoustic pressure and velocity was highlighted here, and it was clarified that there are not many controlling parameters to adjust the phase difference. The engine generated 1.1 W of electricity out of 330 W input heat. Kang et al. [7] constructed a two-stage looped tube engine having two loudspeakers in different configurations; within the loop line and in a branch. This engine used pressurized helium (18 bar) as working gas. The idea was to put a thermoacoustic core in each of the two high impedance zones and a loudspeaker in each of the two low impedance zones, to avoid acoustic losses. The loudspeaker connected at the branch helps to tune and set the acoustic phasing difference (velocity and pressure). A ball valve was introduced as an acoustic load to correct the acoustic field. At 171 Hz working frequency, the maximum generated electric power was 204 Watts at 3.41% thermal-to-electric efficiency and a maximum efficiency of 3.43% was obtained at 183 W electric power.

Four-stage thermoacoustic engines were pioneered by de Blok [8,9]. Four novel engines were built with four identical self-matching stages. Basically, they have low acoustic loss because of lower acoustic dissipation in the resonance and feedback loop. The identical four stages were presented as feasible from the construction point of view because of having identical components per stage. The largest engine in this group is named ThermoAcoustic Power (TAP) generated 1.64 kW of electricity using available waste heat of 20 kW, at working frequency of 40 Hz. Senga and Hasegawa [10] built a four-stage engine similar to the de Blok [9] configuration, using air at atmospheric pressure as working medium. The main difference is that it has one load and hence the cross section area of the regenerators increased with the acoustic power flow direction after the load. The acoustic power generated did not reach 1 W on this rig. Zhang and Chang [11] numerically studied the onset temperature, mean pressure, working gas, hydraulic radius and the number of stages of a four-stage engine similar to the de Blok [9] configuration. The results were used to develop another numerical study, of replacing one of the engine stages with a refrigerator stage by Zhang [12]. The simulation results showed that it can reach a relative Carnot coefficient of performance of 28.5% at a refrigeration temperature of 5˚C.

This paper starts with a description of the design and construction of two stage thermoacoustic engine which generate electricity by running a push-pull linear alternator. Followed by the first performance measurements results of the engine. A model having a developed feedback loop is proposed to reduce the length of the engine. A four-stage engine running two push-pull linear alternator will be given at the end of this paper.

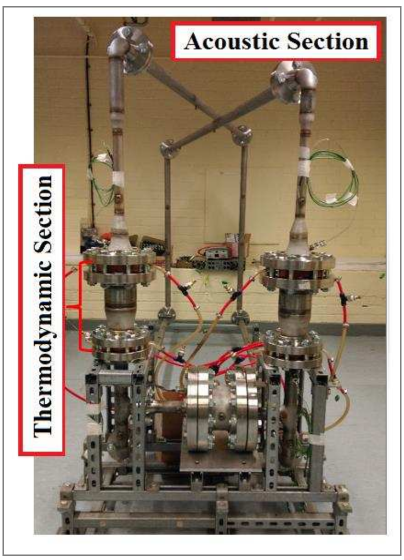

Fig 1. Photograph of the experimental apparatus.

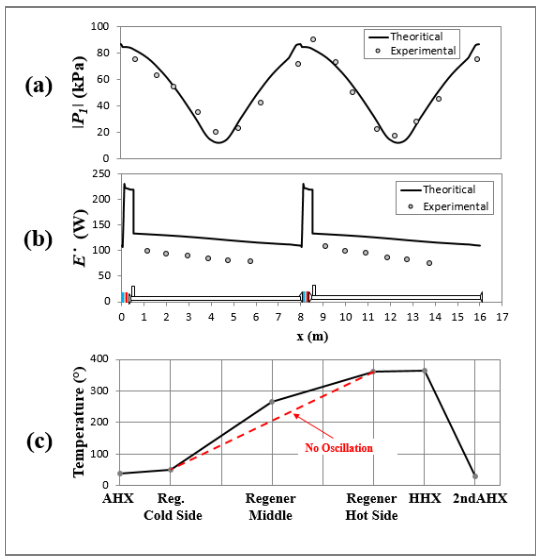

Fig 2. Simulation and experimental results (a) pressure amplitude, (b) acoustic power flow along the engine (c) thermoacoustic core temperature distribution.

2 Experimental Results

The apparatus is a one wavelength, 16.1 m long, looped tube engine filled with 28 bar helium. It consists of two identical stages each having a power extraction point and the linear alternator connecting these two points, as shown in Figure 1. Each stage consists of thermodynamic section where heat is transferred to or from the working gas and acoustic section which comprises of pipes transmitting the acoustic power from one place to another. The details of the rig could be found in [13,14].

The engine runs at a frequency of 54.68 Hz and the optimum load resistance is 30 Ω. The maximum electricity generated was 48.6 W at 2.7% thermal-to-electric efficiency. The regenerator temperature difference was 310 K. The pressure amplitude distribution has been measured in sixteen locations along the engine loop. Additionally, the simultaneous measurement of pressure signals and phase difference between each pair of adjacent transducers allows calculating the acoustic power at the midpoint between adjacent transducers. As shown in Figure 2a, the distribution of the pressure amplitude along the engine shows a good match between the experimental the theoretical results. In addition, Figure 2b compares the experimental acoustic power to the simulation results. Generally, the trend of two results is in agreement, while there is a 20-30% discrepancy in absolute power levels. Figure 2c, shows that all temperature distribution along the thermoacoustic core. The non-linear temperature distribution graph confirms that there is Gedeon streaming, compared to the linear distribution at no oscillation run.

3 Feedback Loop Optimization

The main purpose of the feedback loop is to deliver acoustic power from the end of a stage to the beginning of the other at a convenient acoustic phasing. The built two-stage thermoacoustic engine is 16.1 m long, each stage is 8.05 m long. The feedback loop length of each stage is approximately 7.5 m long. The feedback loop consists of approximately 7.05 m long, 1.5 inch (40.9 mm) diameter pipe, 275 mm long, 1 inch (26.6 mm) diameter pipe, and reducers. This feedback loop could be made shorter by changing the cross-section of the pipes.

Firstly, the feedback loop has been modelled separately investigating a shorter configuration delivering sound at the same phasing. Secondly, the feedback loop of the engine model was changed from the long straight loop to the new short multi-cross-section loop. The length of the previous feedback loop was needed to shift the acoustic phasing of the pressure and volume flow velocity by 180° between stages. This could be achieved by using multi-cross-section feedback loop. The wide cross-section pipe shifts the volumetric flow velocity phase by acting as acoustic compliance, while narrow pipe shifts the pressure phase by acting as acoustic inertance. The combination of compliance-inertance shifts the acoustic phasing in much shorter length. The new proposed feedback loop consists of inertance-compliance-inertance. The first section is a 300 mm long, ½ inch diameter pipe which is part of the previous configuration, followed by a cone leading to 1313 mm long pipe of ¾ inch (20.9 mm) diameter. A non-standard 50 mm long reducer is used to connect the ¾ inch pipe to a 3 inch pipe. A 420 mm long and 3 inch (77.9 mm) diameter pipe acts as an acoustic compliance which shifts the volumetric flow velocity phase with approximately 40°. A non-standard 50 mm long reducer is used to connect the 3 inch compliance to a ⅜ inch inertance. The inertance is a 584 mm long and ⅜ inch diameter pipe which shifts the pressure phase of approximately 62°. The last part is 189 mm reducer (combination of standard reducers) connecting the ⅜ inch pipe to the 4 inch core. The lengths of the two inertances and compliance has been optimized carefully aiming to achieve the acoustic conditions at a shorter length possible. Figure 3 compares the engine configuration for both feedback loops.

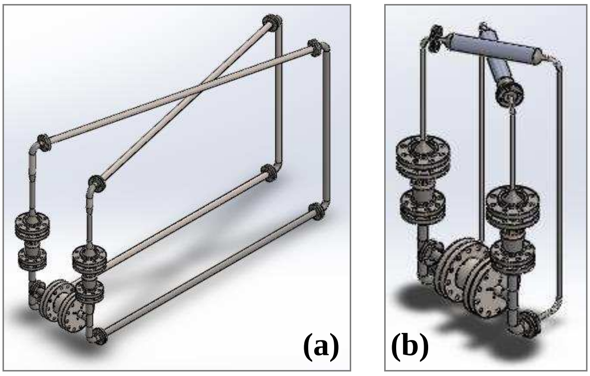

Fig 3. Thermoacoustic engine (a) with previous feedback loop, (b) with proposed feedback loop.

The engine model is 7.5 m long and runs at 56.8 Hz. At a 375 K regenerator temperature difference, the engine generates 130 W of electricity. Figure 4 shows the simulation results of the engine. Figure 4 shows the calculated acoustic power distribution along the engine. Clearly the acoustic power is generated in the regenerators and mainly extracted/dissipated at the linear alternator junctions. The figure shows that the inertance dissipates acoustic power much more than the compliance. Also, the smaller diameter inertance (⅜ inch pipe) dissipates acoustic power more than the bigger diameter (¾ inch) pipe.

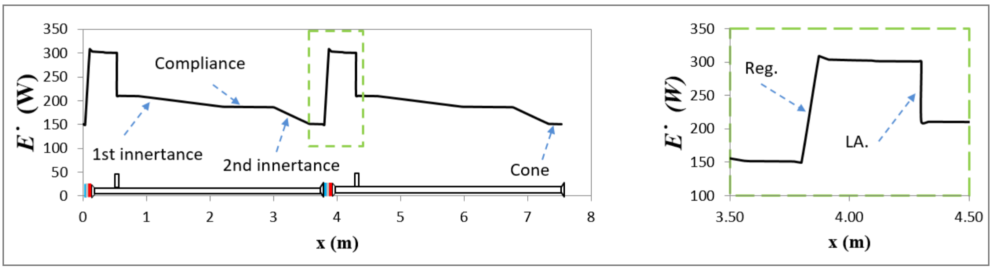

Fig 4. Simulation acoustic power flow along the engine.

4 Four-stage thermoacoustic engine

Basically, the development of the two-stage engine to a four-stage engine involves changing the acoustic section only by adopting the use of acoustic inertance-compliance. All the parts of the thermodynamic section will be kept the same, so that the parts of the current two-stage engine could be used in the next research.

The configuration consists of four identical stages each having a power extraction points, and the linear alternators connecting these four points as shown in Figure 5a. Clearly, there is a power extraction at each stage followed by a feedback loop which leads to the next stage. Theoretically, the flow pressure amplitude and volumetric flow rate of each stage is identical in all the stages. Figure 5b shows a proposed layout of the engine.

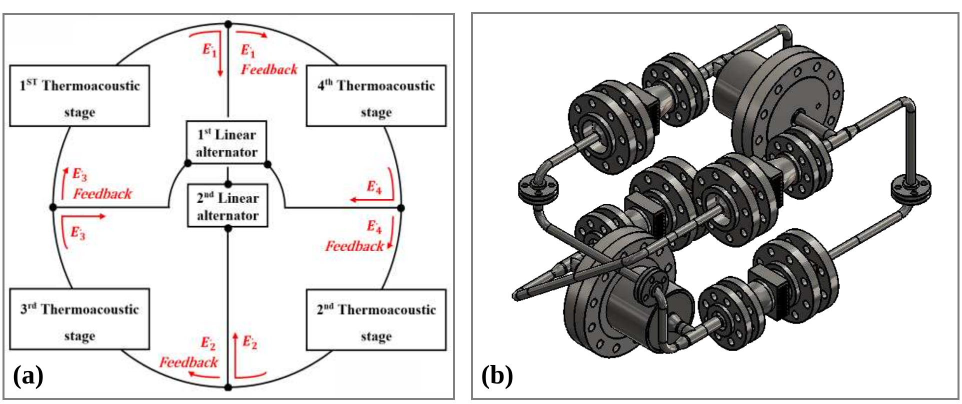

Fig. 5 (a) Conceptual drawing of the proposed four-stage engine, (b) A proposed layout of the four-stage engine.

The modelling was done using DeltaEC package created by the Los Alamos National Laboratory [15]. The DeltaEC shooting method cannot run multi-identical stages. The modelling has been done as a quarter of the engine which is one stage and the other three stages were represented as a self-excited hypothetical flow. There are two self-excited hypothetical flows in this engine, each has a specific flow characterisation based on the understanding of the identical stages and push-pull connection. The first self-excited hypothetical flow is the flow entering the first stage which represents the flow at the end of the fourth stage. The boundary conditions of the this flow were set in the following manner: the temperature, pressure amplitude, volumetric flow rate and total power were set to be equal at the beginning and the end of the simulated stage (at X=0 and X=λ/4), as

$$T_{x=0} = T_{x=\lambda/4} \tag{1}$$

$$|P_{x=0}| = |P_{x=\lambda/4}| \tag{2}$$

$$|U_{x=0}| = |U_{x=\lambda/4}| \tag{3}$$

$$\dot{H}_{2,x=0} = \dot{H}_{2,x=\lambda/4} \tag{4}$$

where T is temperature, P is pressure amplitude, U is volumetric flow, and $\dot{H}_2$ is the total power. The phases of pressure and velocity were set to be shifted by 180°° at the end of the stage with reference to the beginning (at X=0 and X=λ/4), as

$$Ph(P)_{x=0}=Ph(P)_{x=\lambda/4}+180° \tag{5}$$

$$Ph(U)_{x=0}=Ph(U)_{x=\lambda/4}+180° \tag{6}$$

where *Ph(P)* is pressure phase and *Ph(U)* volumetric flow phase.

The second self-excited hypothetical flow is applied to the other side of the linear alternator. The boundary conditions of the second self-excited hypothetical flow were set based on the physics of push-pull operation. The pressure amplitude, volumetric flow and velocity phase were set to be equal on both sides of the alternator piston. Only the pressure phase was set to be out of phase (phase difference of 180˚). The three boundaries were set as targets at locations A and B which are before and after the linear alternator piston, as

$$|P_A|=|P_B| \tag{7}$$

$$\mathrm{Ph(P)_A=Ph(P)_B}+180° \tag{8}$$

$$\dot{H}_{2,A} = \dot{H}_{2,B} \tag{9}$$

As the required acoustic impedance and thermodynamic section dimensions optimization have already been done in the previous design [13,14], the layout and feedback loop is optimised in this part. The optimum feedback loop tube diameter was 10 mm. As explained before in Section 3, the narrow pipe acts as an acoustic inertance and shifts the pressure phase by approximately 75°. There is no need for an acoustic compliance as the volumetric flow velocity phase already shifts at the thermoacoustic core by approximately 65°. A feedback loop of 840 mm was found to be sufficient to match the stages. The simulation optimization introduced the dimensions of the physical parts. Figure 5b shows a proposed layout of the four-stage engine.

The modelling was done using DeltaEC package created by the Los Alamos National Laboratory [15]. Figure 6 shows the simulation results. The graphs on the right are magnified areas marked by green dashed lines of the graphs on the left. Figure 6a shows the calculated pressure amplitude distribution along the engine loop. There are peaks at each regenerator of the four stages. There is a major pressure drop at the regenerator caused by the flow resistance. Figure 6b shows the distribution of volumetric velocity along the thermoacoustic engine. The engine has been designed to have the lowest volumetric flow rate at the regenerator to minimize the viscous dissipation. There is a volumetric flow rate drop at the linear alternator branch caused by the power extraction at the linear alternator.

Figure 6c is the acoustic impedance profile along the engine. It can be seen that the acoustic impedance is nearly maximum at the regenerators which is one of the design strategies. The acoustic impedance drops within the regenerator length, which is caused by the pressure drop and velocity amplification. Figure 6d shows the phase difference between the velocity and pressure oscillation along the engine. This graph illustrates that the phase difference is zero within the regenerator limited which is preferred, and couldn’t be maintained in the previous two-stage design. Figure 5e shows the acoustic power distribution along the engine. Clearly, the narrow feedback loop dissipates a big portion of the generated acoustic power comparing to the previous design.

The simulation considers a heat source at a temperature of internal combustion engine exhaust gases, which is able to maintain a regenerator temperature difference of 375 K. The simulation results showed that the engine ran at 56.6 Hz and the total engine length was 5.2 m. Each alternator generated 130.5 W of electricity, and hence, the engine generated 261 W at the theoretical thermal to electric efficiency of 16.2%.

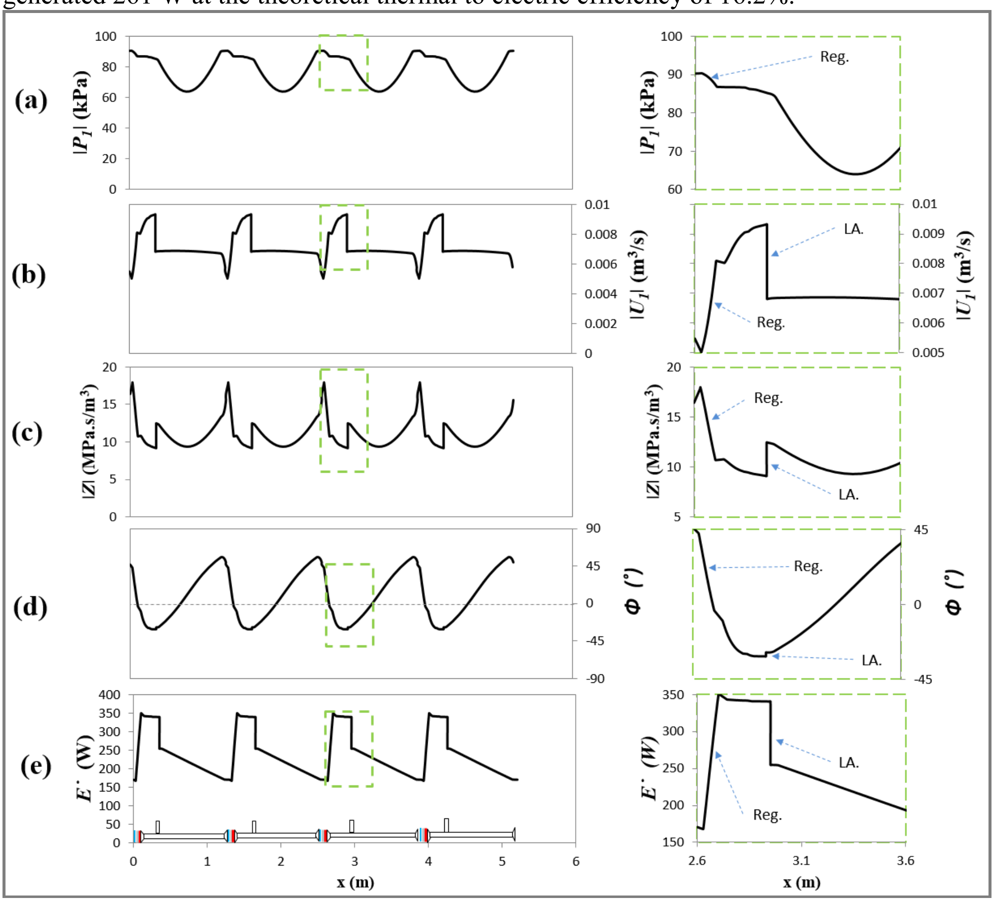

Fig. 6 Simulation results (a) pressure amplitude, (b) volumetric velocity, (c) acoustic impedance, (d) phase difference angle and (e) acoustic power flow along the engine.

5 Conclusion

The experiments showed that the thermoacoustic technology can be used to convert heat at internal combustion engine exhaust gases to useful electricity. A two-stage configuration can run a linear alternator in push-pull mode. The simulation of the feedback loop showed that the feedback loop length could be reduced from approximately 7.5 m to 3.25 m by using a combination of acoustic inertance and compliance. The simulation showed that the engine could be developed from two-stages with one linear alternator to four-stages with two linear alternators. The results illustrated that it ran at 56.6 Hz and the total engine length was 5.2 m. Each alternator generates 130.5 W of electricity, and hence, the engine generates 261 W at the theoretical thermal to electric efficiency of 16.2%.

References

1. R. Bao, G.B. Chen, K. Tang, Z.Z. Jia, and Cao, W.H., Cryogenics, **46**, 666-671 (2006)
2. I.Taymaz, Energy, **31,** 364-371. (2006)
3. V.H Johnson. (No. 2002-01-1969). SAE Technical Paper, (2002)
4. J.S. Jadhao, and D.G. Thombare, Intl. J. of Engineering and Innovative Technology (IJEIT), **2**, 93-100, (2013)
5. T. Yazaki, A. Iwata, T. Maekawa, and A. Tominaga, Phys. Rev. Lett., **81**, 3128, (1998)
6. Y. Kitadani, S.I. Sakamoto, K. Sahashi, and Y. Watanabe, ICA2010, 1-4, (2010)
7. H. Kang, P. Cheng, Z. Yu, and H. Zheng, Appl. Energy, **137**, 9-17, (2015)
8. K. de Blok, Journal of the Acoust. Soc. Am., **123**, 3541-3541, (2008)
9. K. de Blok, In ASME2010, 73-79, (2010)
10. M. Senga, and S. Hasegawa, Appl. Therm Eng, **104**, 258-262, (2016)
11. X. Zhang, and J. Chang, Ener Convers and Manag, **105**, 810-816, (2015)
12. X. Zhang, J. Chang, S. Cai, and J. Hu, Energy Conv. and Manage, **114**, 224-233 (2016)
13. A. Hamood, X. Mao, and A.J. Jaworski, Proceedings of ICR2015, ID531, (2015)
14. A. Hamood, X. Mao, and A.J. Jaworski, Proceedings of IAENG, Vol II, (2016)
15. B. Ward, J. Clark and G. Swift, Design Environment for Low-amplitude Thermoacoustic Energy Conversion DeltaEC, Version 6.3. Los Alamos National Laboratory, (2012)